A New Snow Depth Measurement Technique using ICESat-2 SlideRule in the Western U.S.

Hannah Besso

A thesis

submitted in partial fulfillment of the

requirements for the degree of

Master of Science in Civil Engineering

University of Washington

2022

Committee:

Jessica Lundquist

David Shean

Program Authorized to Offer Degree:

Civil and Environmental Engineering

University of Washington

Abstract

A New Snow Depth Measurement Technique using ICESat-2 SlideRule in the Western U.S.

Hannah Besso

Chair of the Supervisory Committee

Professor Jessica Lundquist

Civil and Environmental Engineering

Snow depth is highly variable across watersheds, yet most snow depth data in the Western U.S. come from sparse point measurements. The water resources community is in need of more spatially representative snow depth data for improved basin-wide snow depth estimates. The NASA ICESat-2 mission is a polar-orbiting laser altimetry satellite launched in October 2018 with the primary goal of measuring ice sheet mass changes at the poles. Previous studies have shown that standard ICESat-2 data products have the potential to provide snow depth measurements of varying accuracy depending on factors such as surface slope and canopy cover. In this study we show that snow depth measurements can be improved using a new on-demand data processing and customization tool named ICESat-2 SlideRule, through which user-specified processing parameters can be used to produce a custom data product optimized for specific scientific aims outside the original goals of the mission. When combined with snow-off Digital Terrain Models (DTMs) from airborne lidar observations, snow-on ICESat-2 SlideRule

observations have the potential to provide a new snow depth dataset across the Western US and the globe. Here we investigate the accuracy of ICESat-2 SlideRule snow depths compared to reference in situ snow telemetry and aerial lidar snow depth observations at two locations with varying terrain characteristics: the upper Tuolumne River watershed, CA and the Methow Valley, WA. We observe strong agreement between the ICESat-2 SlideRule and reference snow depth measurements at both sites, with median residuals of about 0.2 m and 0.4 m in the upper Tuolumne River watershed and the Methow Valley, respectively. Basin-wide aggregation is found to be a better method for ICESat-2 SlideRule calculations than is individual point comparison. Differences in accuracy between sites are attributed to differences in terrain characteristics and the spatial distribution of these characteristics. The ICESat-2 SlideRule data used in this study produced more accurate snow depth results than those found by previous studies using standard ICESat-2 data products in mid-latitude mountainous regions. Therefore, we strongly recommend the use of SlideRule to process ICESat-2 data in such regions and conclude that these data can provide valuable snow depth measurements for areas where high-resolution DTMs are available.

1. Introduction

Melt water from snow and ice accounts for a significant portion of the global hydrologic budget (Huss et al., 2017), and snow acts as a natural water tower that releases streamflow to man-made reservoirs and downstream users throughout the summer (Immerzeel et al., 2020). Knowledge of snow quantity and predictions of when and how quickly it will melt are important for reservoir and agricultural operations. In the western U.S. the majority of snow falls in the mountains, where numerous challenges make snow measurements difficult to obtain.

Various methods for measuring or modeling snow at local and global scales exist, each with their own limitations (Dozier et al., 2016). Due to factors such as the high spatial and temporal variability of mountain snow depth, the ruggedness of weather and terrain in snowy watersheds, and difficulties measuring precipitation amounts and phases, estimating snow in the mountains is currently the most pressing problem in hydrology (Lettenmaier et al., 2015; Durand et al., 2021). The Western U.S. is unique in that it has a relatively dense network of snow telemetry stations that record real-time snow depths and snow water equivalent at point locations throughout the region. These stations provide valuable data to various estimates of distributed snow depth, such as models and snow pattern analysis (Pflug et al., 2022). In places outside the Western U.S., where snow telemetry networks don't exist, snow observations are even more sparse in both time and space. Remote sensing techniques offer some additional snow measurements, but have their own limitations. For example, visible imagery provides snow cover extent in areas without prohibitive cloud cover but does not directly measure snow depth, volume, or water content.

In 2018, NASA launched ICESat-2 with a high resolution lidar instrument on board and the primary goal of measuring small changes in surface elevation at the poles. At high latitudes, change detection can be accomplished directly using differences between chronological ICESat-2 measurements (Magruder et al., 2021; Walker et al., 2021; Sochor et al., 2021; Brunt et al., 2019). At lower latitudes, a lack of repeat ICESat-2 measurements precludes direct change detection, necessitating high-accuracy Digital Terrain Models (DTMs) for baseline measurements.

Although ICESat-2 was not designed to measure snow depth at mid latitudes, several studies have evaluated the utility of the satellite's standard data products for measuring seasonal snow depth by differencing snow-on ICESat-2 elevation measurements from snow-off DTM elevations (Deschamps-Berger et al., 2022; Enderlin et al., 2022; Hu et al., 2021). These have shown that depending on the study site, snow depths can be retrieved from a combination of snow-on ICESat-2 standard data products and snow-off lidar elevation datasets, with accuracies ranging from about 0.20 m to > 1 m (Enderlin et al., 2022). A recent study (Shean et al., 2021) showed improved snow depth retrieval accuracy by utilizing a new on-demand data processing and customization tool named ICESat-2 SlideRule (Swinski et al., 2022). The results show that in mid-latitude areas with very low slope, relatively deep seasonal snow depth, and sparse canopy cover, ICESat-2 SlideRule data products can be used to measure snow depth to a high accuracy.

In the western U.S. most snow falls at high elevations in rugged mountain terrain with varying amounts of canopy cover. ICESat-2 ground elevation accuracies have been found to vary greatly depending on study site characteristics; increases in surface slope and canopy cover have been

found to dramatically decrease ICESat-2 elevation accuracies (Neuenschwander et al., 2020; Hu et al., 2021; Liu et al., 2021; Deschamps-Berger et al., 2022; Zhang et al., 2021; Wang et al., 2021; Enderlin et al., 2022). In this study we evaluate and compare ICESat-2 SlideRule snow depth retrievals in two basins with varying terrain and vegetation characteristics: the upper Tuolumne River watershed in California's Sierra Nevada and the Methow Valley in Washington's eastern Cascade Mountains.

ICESat-2 has the potential to supplement current snow depth measurements, increasing the spatial and temporal distribution of depths that can be used for improving snow modeling and forecasting. If taken beyond the western U.S., ICESat-2 could provide depth measurements in locations that have historically had none.

2. Methods, Instruments, and Study Sites

2.1 ICESat-2

The primary objective of the ICESat-2 mission was to continue polar altimetry measurements to derive ice sheet mass balance and sea ice thickness. Secondary objectives were to provide elevation measurements for mountain glaciers and global vegetation canopy structure (Markus et al., 2017). Notably, these goals did not include snow depth retrievals; but snow is highly reflective at the ICESat-2 laser wavelength of 532 nm (Warren, 2019), resulting in a strong return signal and limited surface penetration in snow (Perovich, 2007).

The Advanced Topographic Laser Altimeter System (ATLAS) is the photon-counting lidar instrument onboard ICESat-2. It operates with 6 parallel beams; 3 "strong" beams and 3 "weak" beams, where weak beams have ¼ the optical power of the strong beams. It has an average orbital altitude of 500 km, and each beam has a footprint diameter of 10.5 - 12 m (Magruder et al., 2020). The instrument was found to have a vertical precision of 0.07 m and a bias of 0.03 m over the flat interior of the Antarctic ice sheet (Brunt et al., 2021), while over flat terrain at mid latitudes it was found to have a vertical RMSE of 0.32 m and a horizontal geolocation RMSE between 0.15 - 1.8 m (Magruder et al., 2020).

In the polar regions, ATLAS acquires data along the same reference ground track every 91 days to allow for precise elevation change measurements. Over non-polar latitudes ATLAS is systematically off-pointed, with the goal of mapping global vegetation structure. This results in greater spatial coverage but fewer systematic repeat measurements (Neumann et al., 2019).

As with any lidar instrument, the accuracy of ICESat-2 decreases under certain conditions. Optically thick clouds and dense vegetation canopy cause fewer photons to reach the ground surface. Steep surface slopes and rugged terrain can lead to higher elevation uncertainty in two ways: small horizontal geolocation errors can become large apparent vertical errors, and the increased spread of photons reduces the precision of each discrete surface return (Deems et al., 2013; Smith et al., 2019).

2.2 Standard ICESat-2 Data Products

The ICESat-2 project distributes several standard data products, including low-level ATL03 products containing classified photons and higher-level products derived from the photon data. Standard products with potential for snow measurements include the Land Ice Height product,

known as ATL06 (Smith et al., 2019; Smith et al., 2021), and the Land and Vegetation Height product, known as ATL08 (Neuenschwander et al., 2019; Neuenschwander et al., 2021).

The ATL06 products are generated over areas containing land ice, including the ice sheets, ice caps and mountain glaciers (Smith et al., 2021). These areas are assumed to be non-vegetated and fairly smooth, with single-degree variations in slope over length scales of hundreds of meters. Linear fits to photon heights are computed along 40 m segments that overlap with neighboring segments, resulting in a point step size of 20 m (Smith et al., 2021). Using this product for other surfaces, such as steep vegetated mountains, can result in large errors due to several factors. The ATL06 elevations are computed for all high-quality photons without differentiation between returns from the canopy or ground surfaces. Furthermore, computing a single elevation for each 40 m segment cannot effectively represent steep or rough terrain. Finally, the ATL06 products are unavailable for mountain ranges without nearby glaciers. Despite these limitations, recent studies have shown that ATL06-derived snow depths have errors of -0.36 m to 0.73 m in the Sierra Nevada, CA (Deschampes-Berger et al., 2022).

The ATL08 products provide ground and canopy heights over 100 m segments based on additional photon-level classification (Neuenschwander et al., 2021). The main purpose of the product is to supply global canopy structure data to estimate global forest biomass and biomass change (Neuenschwander et al., 2022). The ground elevation data from ATL08 are potentially more suitable for snow depth calculations; however, the 100 m segment lengths are problematic for precise elevation change measurements over steep and rugged terrain. ATL08-derived snow depths have shown depth residuals of over 1 m in rugged areas (Enderlin et al., 2022; Hu et al., 2021).

2.3 ICESat-2 SlideRule

The ICESat-2 SlideRule project provides an efficient, cloud-based, on-demand science data processing system for the ICESat-2 mission (Shean et al., 2022; Swinski et al., 2022) . It allows the user to rapidly process the ATL03 photons using the ATL06 algorithm with custom parameters. This customizability is especially useful for applications of ICESat-2 data outside the original scientific aims of the mission; for example, the ATL08 canopy and ground classifications can be used to filter the ATL03 photons, which can then be aggregated for segments with user-defined length.

For this study, we used SlideRule to prepare custom ATL06-SlideRule (ATL06-SR) data products using all available ATL03 granules acquired between October 2018 and May 2022 over our study sites. We computed the average ground surface height over 40 meter segments containing more than 10 high-confidence photons classified as ground returns by ATL08, providing a final step size of 20 m (Table 1).

Table 1
Comparison of ICESat-2 data products for snow depth calculation.

	Segment Length	**Step Size**	**Photon Classification**	**Photon Confidence**
ATL06-SR	40	20	Ground	High
ATL06	40	20	All Land	Medium & High

ATL08	100	50	Ground	Medium & High

2.4 Study Sites

This study focused on two watersheds in the Western U.S. containing high resolution aerial lidar data. Based on previous research (Deschamps-Berger et al., 2022; Hu et al., 2021; Neuenschwander et al., 2020; Treichler and Kääb, 2017), we chose study sites based on their terrain ruggedness, percent canopy cover, and median snow depth accumulation. Terrain ruggedness was assessed by calculating the average slope and Terrain Ruggedness Index (TRI) for the basins across three different length scales. TRI was developed to quantify terrain heterogeneity and is calculated by taking the square root of the sum of squared elevation differences between a target cell and its eight surrounding cells (Riley et al., 1999). Slope and TRI were calculated at a variety of length scales, which were chosen to target fine-scale surface roughness at the sub-ATL06-SR step size (3 m), at the scale of the ATL06-SR step size (20 m), and at the scale of across-track separation between beams within pairs (90 m). Percent canopy cover was calculated by creating a Canopy Height Model (CHM) from the difference between the Digital Terrain Model (DTM) and the Digital Surface Model (DSM) and finding the basin percentage of pixels with canopy cover height greater than 2 m. Basin average snow depth was calculated using snow depth maps derived from Aerial Lidar Surveys (ALS) (Painter and Bormann, 2020) where available (Tuolumne) and Community Snow Observations (https://communitysnowobs.org/snow-data/) where ALS-derived snow depth maps were unavailable (Methow). Study site extents were restricted to existing snow-off high-resolution DTMs. Based on the characteristics listed above, we chose a site where ATL06-SR snow depth calculation methods were expected to perform with high accuracy (i.e., Tuolumne Meadows, CA) and a site that would test the limits of these methods (i.e., Methow Valley, WA) (Fig. 1). Basin characteristics can be found in Table 2.

2.4.1 Upper Tuolumne River Watershed, CA

The upper Tuolumne River watershed was chosen as a site where ATL06-SR snow depth calculation methods were likely to perform well. It is located within Yosemite National Park and supplies water to Hetch Hetchy Reservoir, which serves the city of San Francisco. The upper watershed (above the outlet of Hetch Hetchy) is approximately 1200 km^2, with an elevation range from about 1200 - 4000 m. Watershed snow depths ranged from about 1 - 2.7 m near the timing of peak snow depth during the study years of 2019 - 2022 (Table 2). There was about 31% canopy cover and many clear-sky days during the snow-on period (Table 2). For brevity, the upper Tuolumne River watershed will be referred to as Tuolumne for the remainder of the paper.

2.4.2 Methow Valley, WA

The Methow Valley was chosen as a site that would test the limits of ATL06-SR data. The Methow River is located in northern Washington on the eastern slopes of the Cascade Mountains. It is a tributary of the Columbia River, which produces over 40% of the nation's hydroelectric power (Lillis, K., 2014) and is essential to the irrigation of Eastern Washington farmland. The portion of the Methow Valley included in this study is approximately 1800 km^2 and contains about 44% canopy cover. Watershed snow depths ranged from 0.46 - 0.59 m near the timing of peak snow depth during the study years of 2019 - 2022. Elevation ranges from 400 - 2700 m (Table 2).

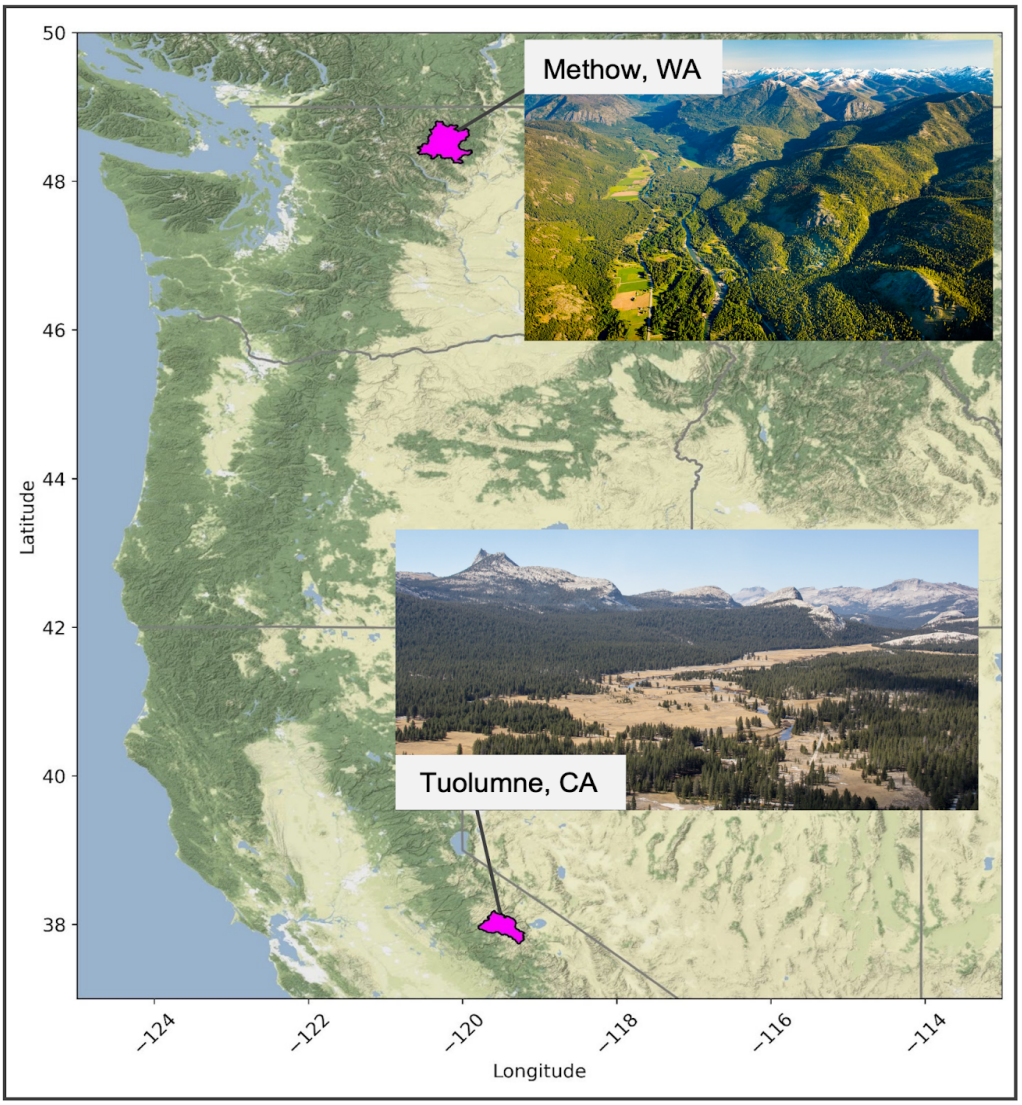

Figure 1. Site locations for the Methow Valley, WA and upper Tuolumne River watershed, CA. Photo credit to Benjamin Drummond/LightHawk and Aron Bosworth.

Table 2
Basin characteristics for the Methow Valley, WA and upper Tuolumne River watershed, CA.

	Basin Median Slope (°) +/- st. dev.	Basin Median TRI (m) +/- st. dev.	% Canopy Cover	Total Area of Lidar Coverage (km^2)	Forest Descriptor	Median Snow Depth (m) | IQR	Elevation Range (m)
Tuolumne	**3 m:** 22 +/- 4 **20 m:** 21 +/- 13 **90 m:** 19 +/- 11	**3 m:** 3 +/- 3 **20m:** 18 +/- 16 **90m:** 87 +/- 54	**3 m:** 31%	1200	Jeffrey pine, western Juniper, western white pine, mountain hemlock, Lodgepole pine*	**2019:** 2.8 | 1.8-3.7 **2020:** 0.9 | 0.1-1.5 **2021:** 1.05 | 0.6-1.3 **2022:** 1.0 | 0.5-1.3	1200-4000
Methow Valley	**3 m:** 21 +/- 11 **20 m:** 20 +/- 10 **90 m:** 18 +/- 9	**3 m:** 10 +/- 6 **20 m:** 19 +/- 12 **90 m:** 258 +/- 129	**3 m:** 44%	1800	shrubstep/grassland, ponderosa pine, douglas fir**	**2019:** 0.6 | 0.4- 0.6 **2020:** 0.5 | 0.3-0.7 **2021:** 0.8 | 0.5 -0.9 **2022:** 0.5 | 0.5-0.7	400-2700

*https://www.nps.gov/yose/learn/nature/plants.htm
**https://www.dnr.wa.gov/publications/lm_hcp_eastside_oldgrowth_guide.pdf

2.5 Airborne Lidar Surveys (ALS)

At each study site, high resolution Digital Terrain Models (DTMs) derived from ALS provided snow-off elevations. In the upper Tuolumne River watershed, a 3 m resolution snow-off DTM and 3 m resolution Lidar Snow Depth products were produced by the Airborne Snow Observatory (ASO) (Painter and Borman, 2020; Painter et al., 2016). The DTM was created from multiple point clouds collected in the summers of 2014, 2015, and 2019; ground return point clouds from each survey were combined to leverage the highest possible point density, resulting in between 1 - 18 points/m^2 (Painter et al., 2016; Currier et al., 2019). No ground control points were used during this survey, as ASO's main concern is geospatial alignment between their own data products rather than absolute georegistration. ASO 3 m Lidar Snow Depth surveys were conducted at various times during the snow-on seasons from 2019 - 2022, with more frequent flights near and after the timing of peak snow depth. The ASO Lidar Snow Depth products were produced by ASO as the difference between the DTM and each ASO 3 m Lidar Snow survey. ASO snow depth products produced using similar methods were found to have mean absolute

errors of < 0.08 m (Painter et al., 2016). The DTM and ASO snow depth products were made available in the local UTM coordinate system and WGS84 ellipsoid (Table 3).

In the Methow Valley, the 1 m resolution snow-off DTM was collected in summer 2018 and was accessed through the Washington Department of Natural Resources's lidar portal (https://lidarportal.dnr.wa.gov/) (Table 3). It had a mean ground return point density of 5.7 points/m^2 and used 83 ground control points (Washington DNR). The DTM was produced in the NAD 1983 Oregon Washington Albers projection with the NAVD88 (GRS 1980) vertical datum and was reprojected to Washington State Plane South prior to being made publicly available. We vertically and horizontally transformed and reprojected this DTM to the local UTM coordinate system and WGS84 ellipsoid (Table 3). At both sites, surface slope and Terrain Roughness Index was computed from the snow-off DTMs at a variety of resolutions for study site characterization (Table 2).

Table 3
Coordinate Reference System (CRS) details and processing steps for DTM sources and ICESat-2 data.

	Original CRS	**Processing Steps**	**Mean Point Cloud Density (pts/m^2)**	**Median Snow-Off Bias from ICESat-2 (m)**
Methow Valley DTM	**Projection:** USFS Region 6 Albers: NAD83 **Vertical Datum:** NAVD88 **Spheroid:** GRS1980 **Units:** meters	1. Reprojected to Washington State Plane South (units: survey feet) by DNR 2. Converted from survey feet to meters 3. Reprojected to UTM Zone 10N: NAVD88 4. Transformed from NAVD88 to WGS84 5. Updated metadata	5.7	-0.44
Tuolumne DTM and ASO Snow Depth Products	**Projection:** UTM Zone 11N **Ellipsoid:** WGS84 **Units:** meters	N/A	?	-0.12
ICESat-2	**Projection:** None **Ellipsoid:** WGS84 based on ITRF 2014 **Units:** meters	1. Projected to local UTM Zone	N/A	N/A

2.6 Observations: Snow Depth Telemetry Sites & CSO

In-situ snow depth measurements were obtained for the duration of the ICESat-2 mission (Oct 2018 - May 2022). In Tuolumne, daily snow depth measurements from the California Data Exchange Center (CDEC) were obtained at the Tuolumne Meadows (2620 m) and Dana Meadow (2965 m) stations. In the Methow Valley, Natural Resources Conservation Service (NRCS) Snow Telemetry (SNOTEL) daily snow depth records were obtained for the duration of the study. No SNOTEL stations were located within the study area, so those within a 35 km radius of the center of the study site were included: Muckamuck and Salmon Meadows stations (1360 m for both stations). To supplement this depth data, we also obtained Community Snow

Observations (CSO) snow depth data from within the study area (https://communitysnowobs.org/participate/).

2.7 ATL06SR Snow Depth Calculations and Bias Correction

High-resolution change detection using separate data sources often requires bias correction due to differences in measurement techniques and small errors introduced by Coordinate Reference System (CRS) transformations. Assuming consistent bias across the ATL06-SR elevations, we conducted a single bias correction for each study site. The DTM elevation was sampled at the coordinates of each ATL06-SR reference point and was then subtracted from the corresponding ATL06-SR elevation. These differences were labeled snow-off or snow-on based on the presence of snow at nearby snow telemetry stations (snow presence defined as snow depths greater than 0.10 m). The median of the snow-off differences at each site was used to bias-correct both snow-off and snow-on differences. For the remainder of the paper, snow-on differences between ATL06-SR and the DTM will be referred to as ATL06-SR snow depths.

ATL06-SR snow depths were aggregated by acquisition date; the sample size for each date depended on the number of ATL06-SR reference points located within the watershed. ATL06-SR snow depths within a radius of each telemetry site were compared to the corresponding snow telemetry depths. In Tuolumne this radius was 5 km; in the Methow Valley it was 20 km to make up for the spatial offset between the snow telemetry stations and the study site. ATL06-SR snow depths for the entire study site were then also compared to each snow telemetry site.

In Tuolumne, the availability of ASO snow depth products enabled a more in-depth analysis of ATL06-SR snow depths. ASO snow depth products were paired with ATL06-SR snow depth data when the two acquisitions occurred within a 20-day timeframe, such that differences between pair member acquisition dates ranged from 2 to 17 days. For each of these pairs, the ASO snow depth data was sampled at the coordinates of the paired ATL06-SR reference points. Two metrics were calculated from the ASO snow depth data: the median snow depth for the entire basin, and the median snow depth of the area sampled by ICESat-2. These metrics were compared to the median snow depth calculated from the corresponding ATL06-SR snow depth data.

3. Results

3.1 Upper Tuolumne Watershed

The median difference between snow-off ATL06-SR elevations and the DTM was -0.12 m (Table 3), which was used to offset both snow-on and snow-off data. The bias-corrected ATL06-SR median snow depths were close to zero in the summer with a positive snow signal in the winter that generally aligned with the snow telemetry depths (Fig. 2).

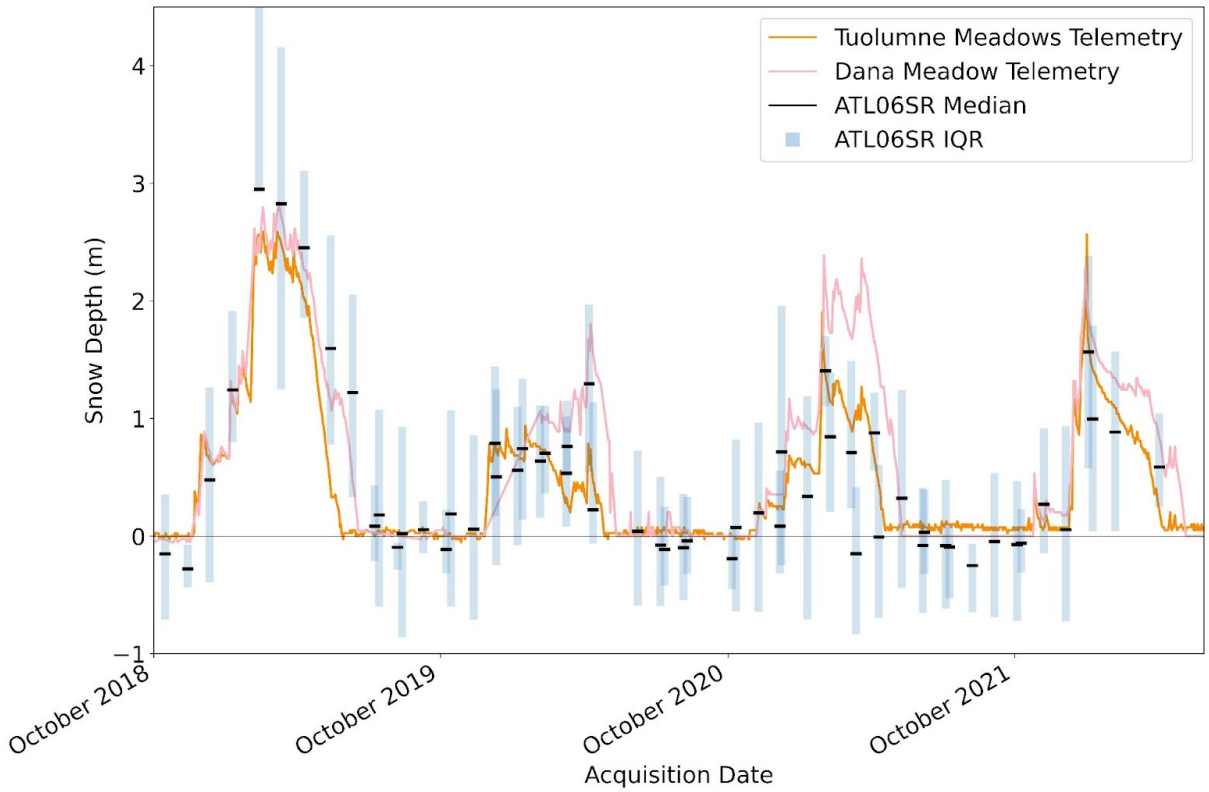

Figure 2. Snow depth values from snow telemetry stations (orange and pink lines) and ATL06-SR snow depth (ATL06-SR minus DTM) distributions within the study area. The light blue boxes indicate the interquartile range, and the black lines indicate the median values for each ATL06-SR acquisition date. Note the tight distribution of ATL06-SR median snow depth values to the telemetry snow depths.

Deeper ATL06-SR snow depths in Tuolumne correspond with higher elevations in the watershed, such as along the watershed's eastern borders (Fig. 3). Lower ATL06-SR snow depths, and in some cases negative snow depths, are apparent in the lower elevations of the watershed, such as along the Grand Canyon of the Tuolumne River in the western center of the watershed, where the Tuolumne River flows into the Hetch Hetchy Reservoir. The distribution of ATL06-SR snow depths follows a generally normal distribution for both snow-on and snow-off values. The spread of data is larger for snow-on values (IQR of 1.57) than for snow-off values (IQR of 1.24). The median of the snow-off ATL06-SR data was 0 m due to the bias correction described in section 2.7, and the median of the ATL06-SR snow depth data was 0.8 m. The higher elevations of the watershed were generally unvegetated or sparsely vegetated, with the majority of canopy cover at lower elevations or in subalpine meadow systems.

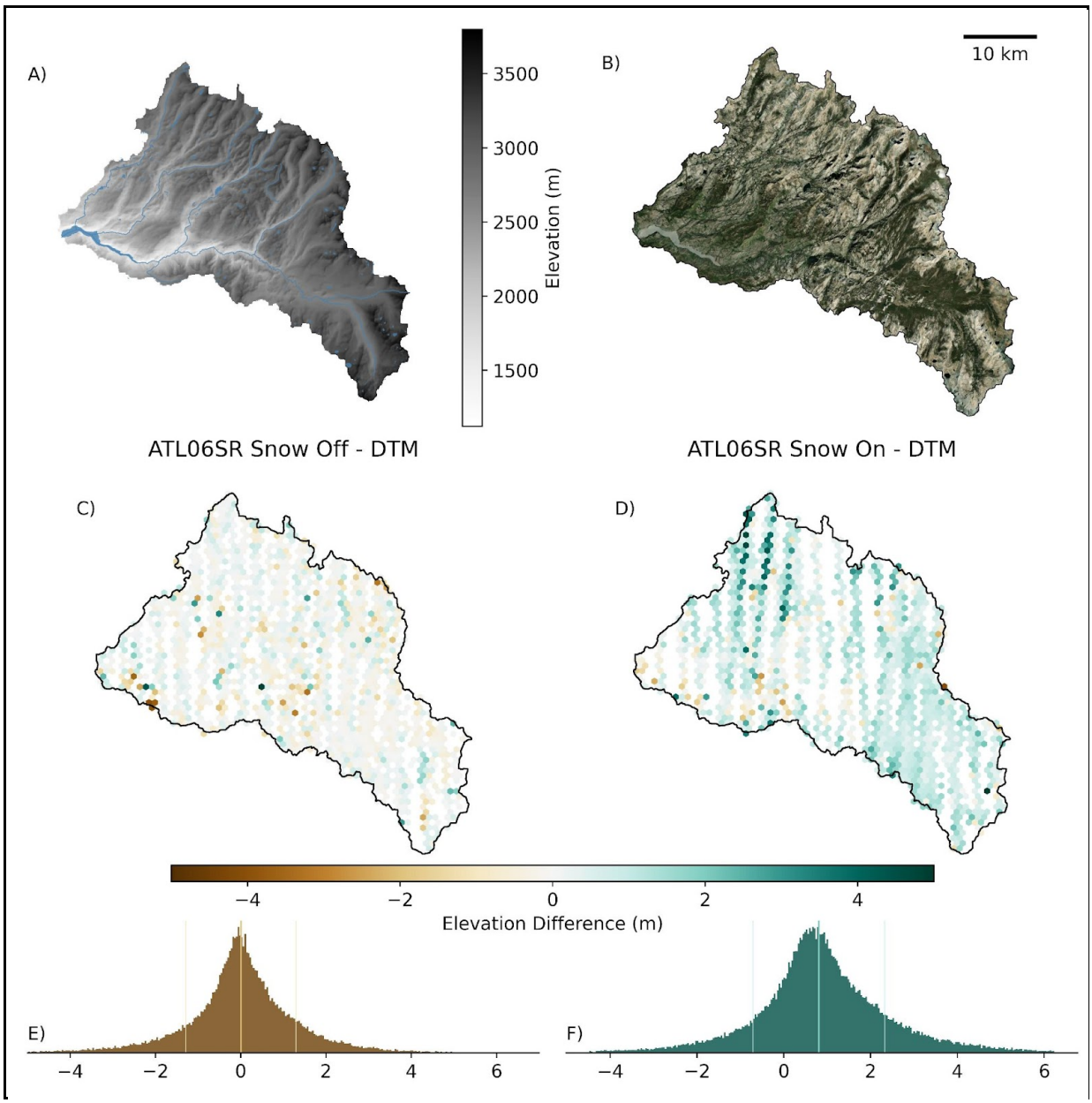

Figure 3. A) Elevation map and hillshade of Tuolumne, with Hetch Hetchy reservoir in the center west of the watershed. B) Snow-off satellite imagery of the watershed. Note the distribution of vegetation at lower elevations and in subalpine meadow zones. C) Heat map of ATL06-SR snow-off differences from the DTM. Note the large number of values close to 0. D) Heat map of ATL06-SR snow depth values. The deepest snow depths occur in the high-elevation northern portion of the watershed and along the high-elevation eastern edges of the watershed. E) Histogram of the ATL06-SR snow-off differences from the DTM. Note that median falls at 0 and the data appears normally distributed. F) Histogram of all the ATL06-SR snow depths. The median falls at about 0.8 m and appears normally distributed.

3.1.1 Comparison of ATL06SR & ASO Snow Depth Pairs

Sampled Pair Comparison: There were eight pairs of ATL06-SR/ASO acquisitions, with temporal offset between pair members ranging from 2 to 17 days (Table S-1). These pair members captured similar median snow depths but different snow depth variabilities, with

ATL06-SR pair members reporting more variability than sampled ASO pair members in all cases. The absolute difference in median snow depth values between pair members was 0.19 m (a median percent difference of 21%), with a range of 0 - 0.44 m (0 - 27% difference) (Table S-1). The spread of the ALT06-SR snow depth data was larger in all cases than that of the sampled ASO data.

Sampled Pair Comparison: ATL06-SR pair members maintained very similar median depths to the ASO basin pair members, although ATL06-SR pair members tended to have higher variability (Fig. 4; Fig. 5). The median difference between ATL06-SR and basin ASO pair members was 0.11 m, with a median percent difference of 15% (Table S-1).

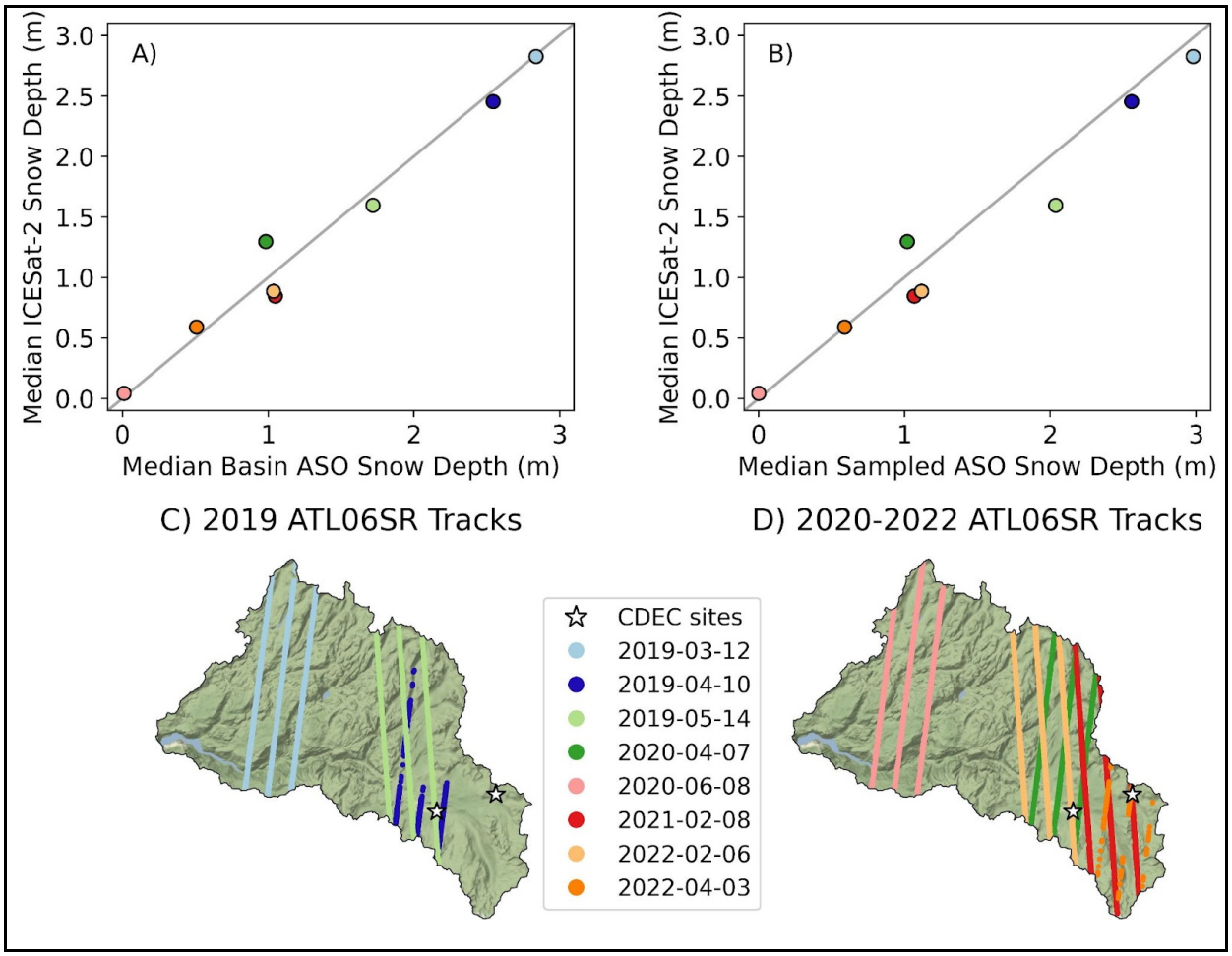

Figure 4. A) ATL06-SR pair member medians aggregated by date, versus snow-on ASO pair member basin-wide medians, colored by the ATL06-SR acquisition date. B) ATL06-SR pair member medians aggregated by date, versus sampled snow-on ASO pair member medians, colored by the ATL06-SR acquisition date. C) ATL06-SR pair member tracks with acquisition dates from 2019. D) ATL06-SR pair member tracks with acquisition dates from 2020-2022, plotted separately from 2019 tracks to avoid overlapping data.

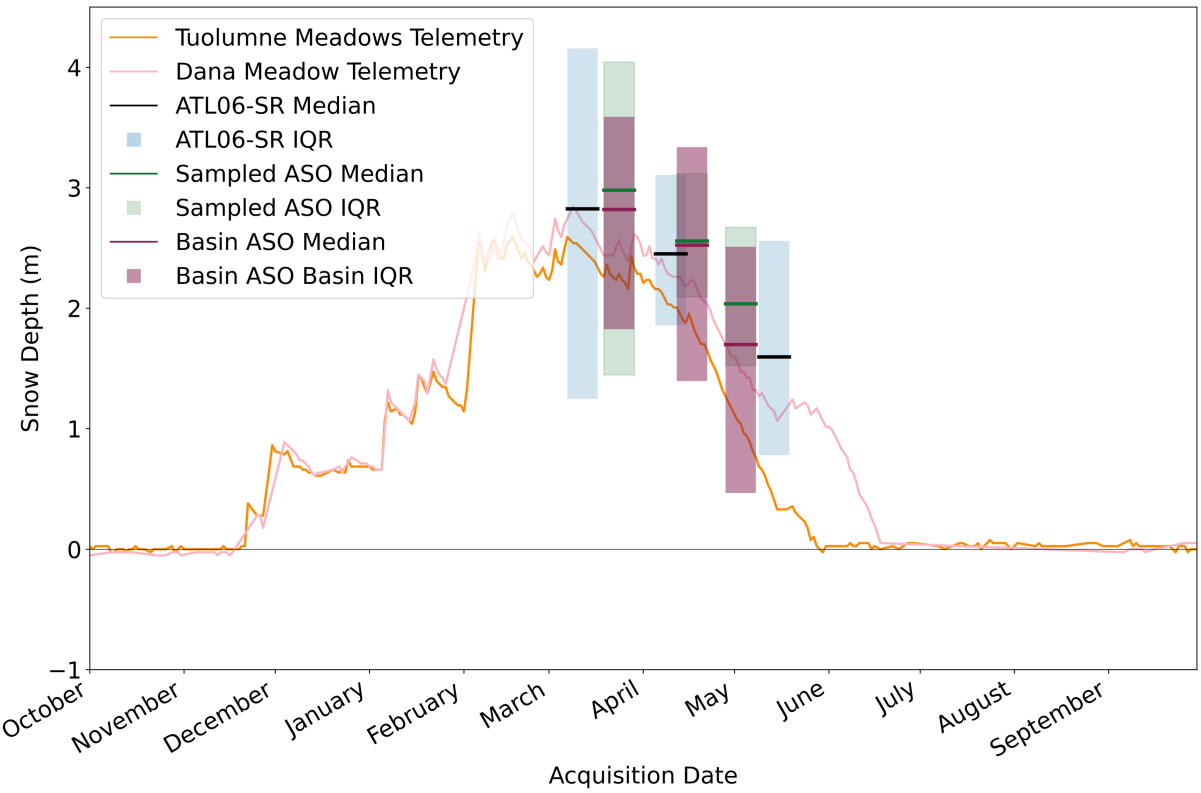

Figure 5. Snow depth values from telemetry stations (orange and pink lines) and ATL06-SR snow depth (ATL06-SR minus DTM) distributions for water year 2019. The light blue boxes and black lines indicate the interquartile range and median snow depth for each ATL06-SR acquisition date in 2019. The light green boxes and green lines indicate the interquartile range and median snow depth for sampled ASO snow depth data. The light pink boxes and pink lines indicate the interquartile range and median snow depth for basin-wide ASO snow depth data.

3.1.2 Comparison of ATL06SR & Telemetered Snow Depth

The median difference between within-radius ATL06-SR depths and the snow depths measured at the Tuolumne Meadows telemetry site was 0.18 m (23%), while the median difference between ATL06-SR from the entire basin and Tuolumne Meadows snow telemetry depths was 0.21 m (28%) (Table 4). The median difference between within-radius ATL06-SR depths and the snow depths measured at the Dana Meadow telemetry site was 0.54 m (45%), while the median difference between ATL06-SR from the entire basin and Dana Meadow snow telemetry depths was 0.46 m (41%). The ATL06-SR data for the entire basin was more variable than the within-radius ATL06-SR data in both cases.

3.2 Methow Valley

In the Methow Valley the median difference between snow-off ATL06-SR and the DTM was -0.44 m (Table 3), which was used to offset both snow-on and snow-off ATL06-SR data. The bias-corrected median ATL06-SR snow depths in the Methow Valley were generally lower than the telemetered and CSO snow depths for that acquisition date (Fig. 5). In the snow-off (summer) season, Methow Valley ATL06-SR median depths were fairly variable, with more extreme positive and negative outliers than in Tuolumne.

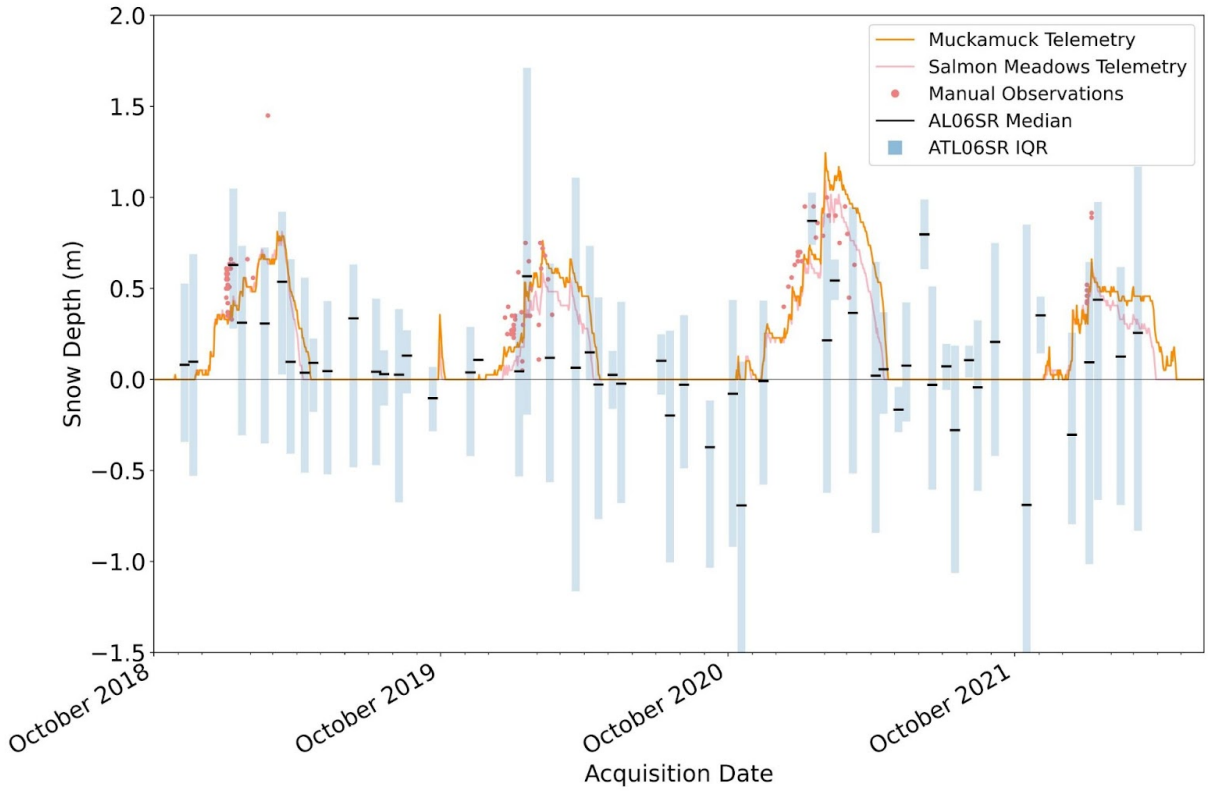

Figure 6. A) Snow depth values from telemetry stations (orange and pink lines) and ATL06-SR snow depth (ATL06-SR minus DTM) distributions within the study area. The light blue boxes indicate the interquartile range and the black lines indicate the median values for each ATL06-SR acquisition date. Note that ATL06-SR median values are generally lower than the telemetered snow depths.

The snow-off ATL06-SR median depth was 0 m, but there were both positive and negative anomalies that appeared to occur on the vegetated steep slopes surrounding the valley bottom (Fig. 6). During the snow-on months, the deepest ATL06-SR depths appeared to occur at high elevations along the western side of the watershed. The median of the ATL06-SR snow depths was 0.18 m, and both the snow-on and snow-off depth histograms appeared less symmetrical than those from Tuolumne. In particular, the snow-off distribution had a heavy negative tail. The spread of the snow depth data was similar to the snow-off data, with IQRs of 1.21 and 1.19 m, respectively. The majority of vegetation occurred on steep slopes to the west of the valley floor.

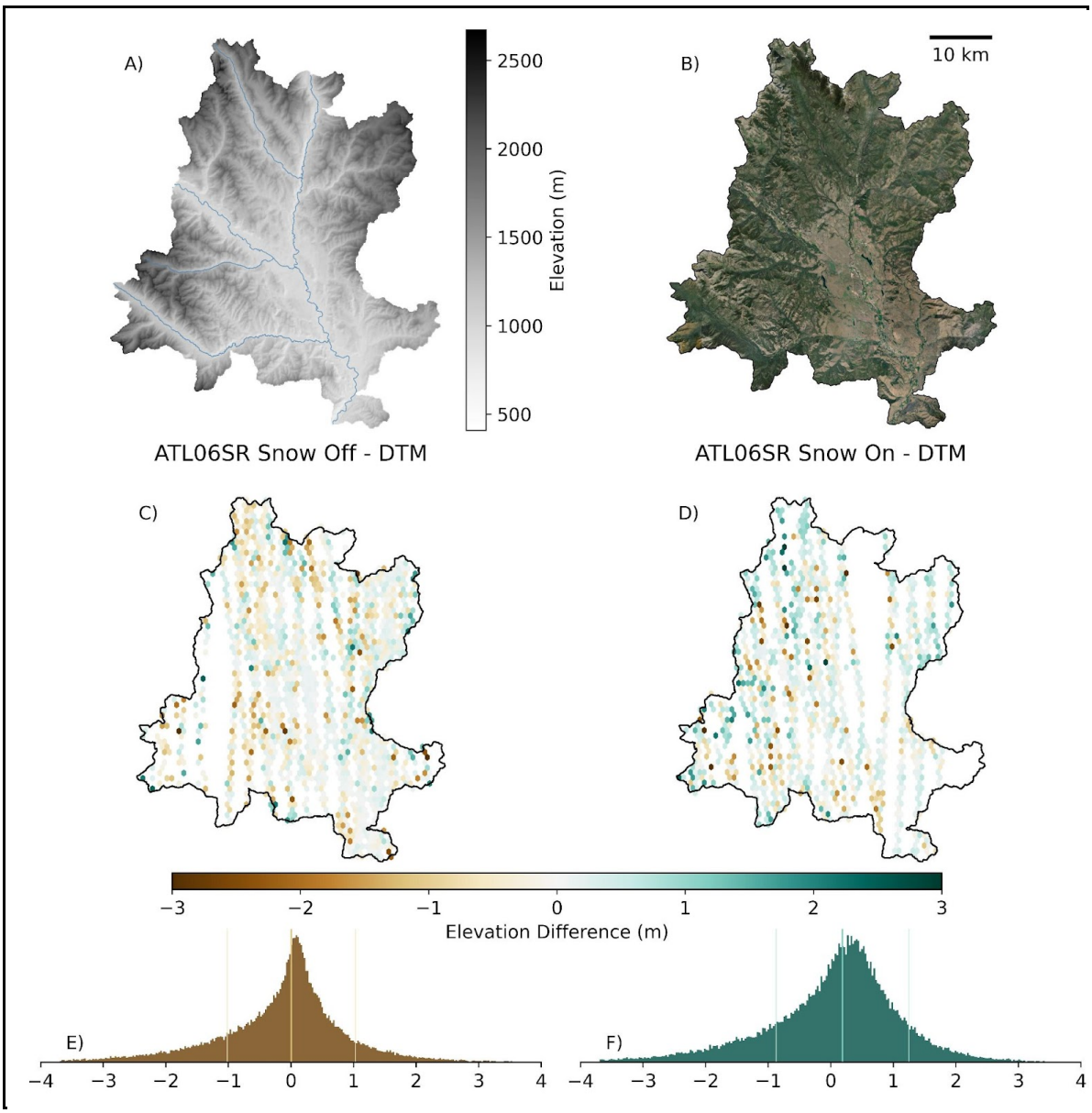

Figure 7. A) Elevation map and hillshade of the Methow Valley. B) Snow-off satellite imagery of the watershed. Note the denser vegetation at higher elevations in the western portion of the basin. C) Heat map of ATL06-SR snow-off differences from the DTM. D) Heat map of ATL06-SR snow depths. Note the deepest snow depths, as well as the most negative depths, in the higher-elevation western portion of the basin. E) Histogram of the ATL06-SR snow-off differences from the DTM. The median difference was 0 m. F) Histogram of the ATL06-SR snow depths. The median falls at about 0.18 m.

3.2.1 Comparison of ATL06SR & Telemetered Snow Depths

The median difference between within-radius ATL06-SR snow depths and the snow depths measured at Muckamuck was 0.34 m (59%) (Table 4). The median difference between ATL06-SR from the entire basin and snow depths measured at Muckamuck was 0.27 m (52%). At Salmon Meadows, the median difference between within-radius ATL06-SR depths and the telemetered snow depths was 0.41 m (62%). The median difference between ATL06-SR from the entire basin and snow depths measured at Salmon Meadows was 0.31 m (61%).

Table 4
Comparison of ATL06-SR snow depths to telemetered snow depths in Tuolumne and the Methow Valley.

Tuolumne	Tuolumne Meadows Radius	Dana Meadows Radius	Basin | Tuolumne Meadows	Basin | Dana Meadows
Median Difference (m)	0.18	0.54	0.21	0.46
Percent Median Difference	23	45	28	41
ATL06SR IQR (m)	0.7	0.74	1.25	
Methow Valley	Muckamuck Radius	Salmon Meadows Radius	Basin | Muckamuck	Basin | Salmon Meadows
Median Difference	0.34	0.41	0.27	0.31
Percent Median Difference	59	62	52	61
ATL06SR IQR	1.41	1.44	1.2	

4. Discussion

4.1 Comparison of ATL06SR & ASO Pairs

Sampled Pairs: There was strong agreement between ATL06-SR and ASO snow-on pairs, with a median percent difference of 20%. In all cases, ATL06-SR snow depths had greater spread than did the sampled ASO snow depths. Snow depth is temporally variable, so we expect that some of the difference between medians was due to the temporal offset between pair members, which ranged from 2 - 17 days. Some of the difference was also likely explained by differences in what the respective lidar instruments "see"; differences in point cloud density, height above ground, and atmospheric interference play a role in the detection of the ground surface.

Basin Pairs: The agreement between ATL06-SR snow depth medians and the ASO basin medians was quite strong, with a median percent difference of 15%, and a median difference of 0.11 m. This presents a compelling argument for the potential use of ATL06-SR aggregated snow depth data for determining basin-wide metrics. Based on the random distribution of ATL06-SR errors and the strong agreement between basin-wide median values, it appears that basin-wide aggregation is a better method for working with ATL06-SR data than is individual point comparison.

4.2 Comparison of ATL06SR & Telemetered Snow Depths

4.2.1 Radius Analysis

The median percent differences for within-radius versus basin-wide snow depths for both Tuolumne telemetry stations were within 5% of each other. The percent median differences for within-radius versus basin-wide data for both Methow Valley telemetry stations were within 7% of each other. The Methow Valley telemetry stations were not located within the study area, which might explain the greater percent differences in the Methow Valley than in Tuolumne. These results suggest that for both sites there was not a significant advantage to restricting the

analysis to locations close to the telemetry stations; basin-wide analyses did not differ much from the radius analyses.

4.2.2 Basin Analysis

Methow Valley median ATL06-SR snow depths were consistently lower than telemetry depths. Both Methow Valley telemetry stations were located at around 1360 m, whereas the median elevation of ATL06-SR data was 1060 m, so the majority of ATL06-SR data were located at lower elevations and therefore were likely measuring lower snow depths than were present at the telemetry stations. Canopy cover tended to increase with elevation in the Methow Valley, so where ATL06-SR did measure snow at higher elevations, those measurements were likely more affected by vegetation than those at lower elevations where snow depth is also lower. The spatial offset between the telemetry stations and the study area likely contributed to differences between the two. Also, the stations were located in high elevation clearings, which frequently are not representative of the median snow depth in surrounding areas (Meromy et al., 2012).

4.3 Study Site Comparison

Both sites had negative bias in ATL06-SR snow-off differences from the DTM, with medians of -0.12 m and -0.44 m in Tuolumne and the Methow Valley, respectively, indicating that ATL06-SR tends to underestimate surface elevations compared to DTM elevations. Enderlin et al. (2022) found that snow-off ATL06 data underestimated surface elevations as well, with a median bias of -0.76 m; note that the magnitude of the ATL06 bias was larger than that of the ATL06-SR data in this study. Within this study, there were fewer negative outliers and better alignment with snow telemetry measurements in Tuolumne than in the Methow Valley, a finding which was consistent with the predictions of our study design. This is likely due to differences in DTM accuracy and study site characteristics such as canopy cover, magnitude of snow depths, terrain roughness, and the dominant orientation of elevational gradients (Table 2). The spatial distribution of these characteristics is also important to consider and is discussed below.

4.3.1 DTM Accuracy

ATL06-SR snow depth calculations in this study relied heavily on high-accuracy DTMs, and DTM accuracy can differ considerably based on the density of the source point cloud. The Methow Valley DTM was produced from a point cloud obtained during summer leaf-on conditions in a region with dense canopy and rough terrain that consistently poses challenges for lidar vendors; the Tuolumne point cloud was also obtained during summer and fall leaf-on conditions, but in a region with sparse canopy and smoother terrain. The dense canopy in the Methow likely decreased both the likelihood of lidar point returns from the ground surface and the accuracy of the ground surface statistics. For this and other reasons related to flight and instrument specifications, the Methow Valley point cloud was less dense than the Tuolumne point cloud, which translated to larger errors in the Methow Valley DTM. Errors on the order of tens of meters were found over cliff faces in the Methow Valley DTM, and in valley bottoms shrubs were consistently misclassified as ground surface (DNR Washington Geologic Survey). Errors in the DTM were propagated to the ATL06-SR snow depths. Large infrequent errors such as those found over cliffs likely had little effect on ATL06-SR median snow depths due to the robustness of median statistics to outliers. However, consistent misclassification of valley shrubs as ground likely positively biased the Methow Valley ground elevation and potentially

contributed to the shallower ATL06-SR snow depths as compared to telemetered snow depths (Hopkinson et al., 2014).

4.3.2 Vegetation Density

The Methow Valley had about 13% more canopy cover than did Tuolumne, and the canopy structure was denser than in Tuolumne (Table 2). This denser canopy likely obscured the ground surface, decreasing confidence in ground elevation values. ATL08 terrain estimates were found to be most accurate at a percent canopy cover of less than 40% (Neuenschwander et al., 2020). The Methow Valley exceeded this threshold, indicating that more canopy-related errors should be expected at this site. The spatial distribution of canopy cover is likely also an important factor. In the Methow Valley, canopy cover is denser at higher elevations, whereas in Tuolumne higher elevations tend to have sparser canopy cover than at lower elevations. Since snow depth tends to increase with elevation at these sites, ATL06-SR measurements of deeper snow depths are likely more accurate in Tuolumne than in the Methow Valley.

4.3.3 Snowpack Depth

Tuolumne consistently has a deeper snowpack than the Methow Valley, providing a stronger signal for ATL06-SR snow measurements and decreasing the percent error for residuals of a certain magnitude. In addition to having a shallower snowpack, the Methow Valley also receives more mixed rain-snow events, which results in greater elevational variation in snow depth as compared to Tuolumne, much of which lies above the snow line. More spatial variability of snow depths in the Methow Valley results in less representative basin medians for specific ATL06-SR tracks and more difficulty in comparing point SNOTEL observations with track medians.

4.3.4 Terrain Roughness

The terrain roughness in the Methow Valley was threefold greater than in Tuolumne at the 3 m and 90 m length scales, which likely contributed to the propagation of horizontal errors to vertical errors and decreased the clarity of the ground surface. The surface slope at all length scales was similar between the sites, suggesting that differences in ATL06-SR elevational accuracy between the sites was due more to terrain roughness than to surface slope angles.

4.3.5 Terrain Orientation

Two different terrain orientation characteristics likely played a role in the different results at the two sites. The first of these was the distribution of elevations related to terrain roughness. In Tuolumne, rougher terrain tended to occur at lower elevations such as in the Grand Canyon of the Tuolumne, where snow tends to be sparse. The higher elevations where snow depths tend to be deeper display smoother terrain, making median snow easier to measure in locations that receive representatively deep snow depths. In the Methow Valley, higher elevations that tend to receive deeper snow depths are more rugged and have more canopy cover. Lower elevations that tend to receive shallower snow depths are smoother and less vegetated. As mentioned previously, these lower elevation valley bottoms displayed misclassified shrubs in the DTM, which likely further decreased the snow depths calculated over these areas. Therefore, the terrain that resulted in the most accurate ATL06-SR measurements in the Methow Valley held shallower snow depths than the rest of the basin.

The second terrain orientation characteristic was the dominant orientation of elevational gradients relative to the north-south orientation of ICESat-2 tracks. In Tuolumne, north-south ICESat-2 tracks tended to capture a variety of elevations, including high elevation regions with deeper snow depths, resulting in ATL06-SR snow depths that were representative of basin snow depths. Within the Methow Valley study area, the elevational gradient was generally oriented east-west, resulting in ICESat-2 tracks that tended to capture a subset of elevations instead of a distribution representative of the basin, which translated to ATL06-SR snow depths that were less representative of basin snow depths.

4.4 Bias Correction

Both sites had negative snow-off differences as compared to the reference DTMs. In addition to the other factors listed in this section, it is likely that the surface reflectance signatures of bare ground versus snow cover impacted the accuracy of the measurements during different seasons. Snow is much more reflective at the ICESat-2 wavelength of 532 nm than is bare ground or vegetation, resulting in a greater number of photon events and better defined ground surface elevations during the snow-on season. The bias correction described in section 2.7 relied on the median difference between snow-off ATL06-SR elevations and the DTM. If this median difference was not temporally consistent across all seasons, it is possible that this bias correction was a source of error for the ATL06-SR snow depth calculations.

4.5 Geospatial Errors

Elevation change detection calculations rely on accurate horizontal and vertical alignment between datasets. The datasets used in this study were produced by different entities and in different CRSs, which likely contributed small errors to the ATL06-SR snow depth calculations. Each dataset was transformed into the same CRS to allow for calculations between datasets; however, CRS transformations themselves can introduce small geolocation errors that propagate through each transformation step. The ATL06-SR elevation data for both study sites was horizontally projected, and the Methow Valley DTM was horizontally reprojected twice (once by the Washington DNR and again by the authors of this study); each horizontal transformation likely introduced small geolocation errors. The Methow Valley DTM was also transformed from the NAVD88 geoid to the WGS84 ellipsoid. Due to deterioration of the geodetic survey markers that define the NAVD88 geoid, this datum is biased by about a half meter and is tilted by about 1 m from the east to west coasts of North America (National Geodetic Survey, 2021). Transformation from NAVD88 to WGS84 can account for most of these errors, but some geolocation errors on the order of 0.15 m (NOAA) can propagate to the transformed dataset. Geolocation errors resulting from this datum shift were likely the largest of all the transformations in this study, so the Methow Valley DTM likely had the largest geolocation errors resulting from CRS transformations. These errors are especially problematic in rough terrain where small horizontal errors at a given location can translate to large vertical errors and affect the accuracy of ATL06-SR snow depth calculations. Therefore, high quality DTMs produced in reference to the WGS84 ellipsoid are necessary to produce accurate ATL06-SR snow depth calculations.

5. Conclusions

This study investigated the use of customized ICESat-2 SlideRule data products for snow depth measurements during water years 2019 - 2022 at two study sites in the western U.S.. It showed

that aggregation of ATL06-SR snow depths provides accurate median basin snow depth at scales of 1000 - 2000 km^2. Differences in snow depth measurement accuracy between sites are attributed in part to the spatial distribution of site characteristics including canopy cover, magnitude of snow depths, terrain roughness, and the dominant orientation of elevational gradients relative to ICESat-2 track orientations. The upper Tuolumne River watershed provides the ideal location for the initial testing of new remote sensing snow measurement techniques due to favorable terrain characteristics and the availability of ASO 3-m Lidar Snow Depth products. Other snow-covered areas that are more challenging for remote sensing techniques, such as the Methow Valley, are often overlooked despite making significant contributions to regional water budgets. The lack of existing snow products in these regions means that the availability of ICESat-2 SlideRule snow measurements is especially impactful.

One current limitation of ICESat-2 measurements for surface change detection is the need for baseline measurements from high-resolution snow-off DTMs. As discussed in section 4.3, DTM quality is dependent on the density of source point clouds, and the combination of DTMs with ICESat-2 data is most accurate when DTMs are produced within a few years of study timing and in reference to the WGS84 ellipsoid. Therefore, not all lidar products are created equal, and snow depth calculations should only be conducted using the highest quality lidar products. This limits the regions where ICESat-2 can be used to measure snow depth. The USGS 3D Elevation Program is committed to providing nationwide DTMs by 2023, which should make ICESat-2 snow depth measurements possible throughout snow covered regions of the U.S. as long as lidar quality is sufficiently high. However, one of the most appealing components of ICESat-2 data is its global coverage, and high-resolution DTMs are not publicly available in many of the snow-covered regions of the world (i.e. High Mountain Asia). To utilize the full potential of ICESat-2 data, new aerial lidar surveys should be focused in regions without existing high quality data. Additionally, future work should focus on new ways to directly calculate snow depth from ICESat-2 (Hu et al., 2022), and the snow community should advocate for systematic repeat ICESat-2 measurements over snow-covered regions to eliminate dependence on high quality DTMs.

Terrain characteristics should be considered in decisions of where and how to use ATL06-SR snow depth products, with ideal sites containing moderate surface roughness and canopy cover, and snow depths greater than a half meter. Additional factors to consider include the availability of ICESat-2 measurements at a given location and appropriate aggregation length scales. ICESat-2 measurement density increases with latitude, so lower latitude study sites will need to be large enough to include a sufficient sample size. Study sites will also need to be small enough for median snow depth statistics to remain representative, which likely varies based on terrain and local synoptic storm scales; but further research is needed to determine mountain range correlation lengths.

The customized ATL06-SR data used in this study outperformed standard ICESat-2 data products in mid-latitude mountainous terrain, and produced snow depth measurements within 20% of aerial lidar snow depth products. For this reason, we strongly recommend the use of ICESat-2 SlideRule (Shean et al., 2022) for snow depth measurements in these regions. This product has the potential to provide a highly accurate, temporally infrequent snow depth dataset with the potential for assimilation into distributed snow water equivalent (SWE) models and

multidecadal snow reanalysis patterns for significantly improved global SWE estimates (Margulis et al., 2019; Pflug et al., 2019). ICESat-2 could continue collecting data through the end of the decade and with a little planning could become a functional operational forecast tool for water managers. For this to happen, high accuracy snow-off aerial lidar surveys would need to be produced in large-scale basins and in global datums to provide baseline measurements. ICESat-2 data would need to be made publicly available on the scale of one week instead of multiple months. Finally, ICESat-2 managers could implement repeat track mode over key water resource regions such as the Sierra Nevada, with measurements timed for near peak snow depth. Currently no single snow measurement product provides complete snow information in the Western U.S., and certainly not at a global scale. New products and assimilation techniques are necessary to improve water resource management (Bureau of Reclamation, 2021), and ICESat-2 SlideRule should be one of the tools implemented in this effort.

Author Contributions

Hannah Besso: Conceptualization, Investigation, Methodology, Visualization, Writing – original draft, Writing – review & editing.
Jessica D. Lundquist: Conceptualization, Proposal Writing, Writing – review & editing, Supervision.
David Shean: Conceptualization, Writing – review & editing, Supervision.

Declaration of Competing Interest

The authors declare that they have no known competing financial interests or personal relationships that could have appeared to influence the work reported in this paper.

Acknowledgements

We would like to thank the Mountain Hydrology Research group for their comments and feedback on the manuscript. Additionally, we would like to thank the creators of SlideRule for providing technical assistance and for their responsiveness to scientist feedback to make the tool as user-friendly as possible. We gratefully acknowledge funding support from NASA grant 80NSSC20K1293 and the Steve and Sylvia Burges Endowed Presidential Fellowship in Civil and Environmental Engineering.

References

Brunt, K.M., Neumann, T.A., Smith, B.E., 2019. Assessment of ICESat-2 Ice Sheet Surface Heights, Based on Comparisons Over the Interior of the Antarctic Ice Sheet. Geophysical Research Letters 46, 13072–13078. https://doi.org/10.1029/2019GL084886

Brunt, K.M., Smith, B.E., Sutterley, T.C., Kurtz, N.T., Neumann, T.A., 2021. Comparisons of Satellite and Airborne Altimetry With Ground-Based Data From the Interior of the Antarctic Ice Sheet. Geophysical Research Letters 48, e2020GL090572. https://doi.org/10.1029/2020GL090572

Bureau of Reclamation, 2021. Emerging Technologies in Snow Monitoring. Report to Congress. https://www.usbr.gov/research/docs/news/Emerging_Snow_Monitoring_Report_508.pdf

Currier, W.R., Pflug, J., Mazzotti, G., Jonas, T., Deems, J.S., Bormann, K.J., Painter, T.H., Hiemstra, C.A., Gelvin, A., Uhlmann, Z., Spaete, L., Glenn, N.F., Lundquist, J.D., 2019. Comparing Aerial Lidar Observations With Terrestrial Lidar and Snow-Probe Transects

From NASA's 2017 SnowEx Campaign. Water Resources Research 55, 6285–6294. https://doi.org/10.1029/2018WR024533

Deems, J.S., Painter, T.H., Finnegan, D.C., 2013. Lidar measurement of snow depth: a review. Journal of Glaciology 59, 467–479. https://doi.org/10.3189/2013JoG12J154

Deschamps-Berger, C., Gascoin, S., Shean, D., Besso, H., Guiot, A., López-Moreno, J.I., 2022. Evaluation of snow depth retrievals from ICESat-2 using airborne laser-scanning data. The Cryosphere Discussions 1–17. https://doi.org/10.5194/tc-2022-191

Dozier, J., Bair, E., Davis, R., 2016. Estimating the spatial distribution of snow water equivalent in the world's mountains. WIREs Water 3, 461-474. https://wires.onlinelibrary.wiley.com/doi/full/10.1002/wat2.1140

Durand, M., Barros, A., Dozier, J., Adler, R., Cooley, S., Entekhabi, D., Forman, B.A., Konings, A.G., Kustas, W.P., Lundquist, J.D., Pavelsky, T.M., Rodell, M., Steele-Dunne, S., 2021. Achieving Breakthroughs in Global Hydrologic Science by Unlocking the Power of Multisensor, Multidisciplinary Earth Observations. AGU Advances 2, e2021AV000455. https://doi.org/10.1029/2021AV000455

Enderlin, E.M., Elkin, C.M., Gendreau, M., Marshall, H.P., O'Neel, S., McNeil, C., Florentine, C., Sass, L., 2022. Uncertainty of ICESat-2 ATL06- and ATL08-derived snow depths for glacierized and vegetated mountain regions. Remote Sensing of Environment 283, 113307. https://doi.org/10.1016/j.rse.2022.113307

Hopkinson, C., Sitar, M., Chasmer, L., Treitz, P., 2004. Mapping Snowpack Depth beneath Forest Canopies Using Airborne Lidar. Photogrammetric Engineering & Remote Sensing 70, 323–330. https://doi.org/10.14358/PERS.70.3.323

Hu, X., Hao, X., Wang, J., Huang, G., Li, H., Yang, Q., 2021. Can the Depth of Seasonal Snow be Estimated From ICESat-2 Products: A Case Investigation in Altay, Northwest China | IEEE Journals & Magazine | IEEE Xplore [WWW Document]. URL https://ieeexplore.ieee.org/abstract/document/9440674 (accessed 5.11.22).

Hu, Y., Lu, X., Zeng, X., Stamnes, S.A., Neuman, T.A., Kurtz, N.T., Zhai, P., Gao, M., Sun, W., Xu, K., Liu, Z., Omar, A.H., Baize, R.R., Rogers, L.J., Mitchell, B.O., Stamnes, K., Huang, Y., Chen, N., Weimer, C., Lee, J., Fair, Z., 2022. Deriving Snow Depth From ICESat-2 Lidar Multiple Scattering Measurements. Frontiers in Remote Sensing 3.

Huss, M., Bookhagen, B., Huggel, C., Jacobsen, D., Bradley, R. s., Clague, J. j., Vuille, M., Buytaert, W., Cayan, D. r., Greenwood, G., Mark, B. g., Milner, A. m., Weingartner, R., Winder, M., 2017. Toward mountains without permanent snow and ice. Earth's Future 5, 418–435. https://doi.org/10.1002/2016EF000514

Immerzeel, W.W., Lutz, A.F., Andrade, M., Bahl, A., Biemans, H., Bolch, T., Hyde, S., Brumby, S., Davies, B.J., Elmore, A.C., Emmer, A., Feng, M., Fernández, A., Haritashya, U., Kargel, J.S., Koppes, M., Kraaijenbrink, P.D.A., Kulkarni, A.V., Mayewski, P.A., Nepal, S., Pacheco, P., Painter, T.H., Pellicciotti, F., Rajaram, H., Rupper, S., Sinisalo, A., Shrestha, A.B., Viviroli, D., Wada, Y., Xiao, C., Yao, T., Baillie, J.E.M., 2020. Importance and vulnerability of the world's water towers. Nature 577, 364–369. https://doi.org/10.1038/s41586-019-1822-y

Lettenmaier, D.P., Alsdorf, D., Dozier, J., Huffman, G.J., Pan, M., Wood, E.F., 2015. Inroads of remote sensing into hydrologic science during the WRR era. Water Resources Research 51, 7309–7342. https://doi.org/10.1002/2015WR017616

Lillis, K., 2014. The Columbia River Basin provides more than 40% of total U.S. hydroelectric generation [WWW Document]. U.S. Energy Information Administration. URL https://www.eia.gov/todayinenergy/detail.php?id=16891 (accessed 6.8.22).

Liu, A., Cheng, X., Chen, Z., 2021. Performance evaluation of GEDI and ICESat-2 laser altimeter data for terrain and canopy height retrievals. Remote Sensing of Environment 264, 112571. https://doi.org/10.1016/j.rse.2021.112571

Magruder, L., Neumann, T., Kurtz, N., 2021. ICESat-2 Early Mission Synopsis and Observatory Performance. Earth and Space Science 8, e2020EA001555. https://doi.org/10.1029/2020EA001555

Magruder, L.A., Brunt, K.M., Alonzo, M., 2020. Early ICESat-2 on-orbit Geolocation Validation Using Ground-Based Corner Cube Retro-Reflectors. Remote Sensing 12, 3653. https://doi.org/10.3390/rs12213653

Margulis, S., Yiwen, F., Dongyue, L., Lettenmaier, D., Konstantinos, A., 2019. The Utility of Infrequent Snow Depth Images for Deriving Continuous Space-Time Estimates of Seasonal Snow Water Equivalent. Geophysical Research Letters 49, 5331-5340. https://doi.org/10.1029/2019GL082507

Markus, T., Neumann, T., Martino, A., Abdalati, W., Brunt, K., Csatho, B., Farrell, S., Fricker, H., Gardner, A., Harding, D., Jasinski, M., Kwok, R., Magruder, L., Lubin, D., Luthcke, S., Morison, J., Nelson, R., Neuenschwander, A., Palm, S., Popescu, S., Shum, C., Schutz, B.E., Smith, B., Yang, Y., Zwally, J., 2017. The Ice, Cloud, and land Elevation Satellite-2 (ICESat-2): Science requirements, concept, and implementation. Remote Sensing of Environment 190, 260–273. https://doi.org/10.1016/j.rse.2016.12.029

Meromy, L., Molotch, N.P., Link, T.E., Fassnacht, S.R., Rice, R., 2013. Subgrid variability of snow water equivalent at operational snow stations in the western USA. Hydrological Processes 27, 2383–2400. https://doi.org/10.1002/hyp.9355

Neuenschwander, A., Guenther, E., White, J.C., Duncanson, L., Montesano, P., 2020. Validation of ICESat-2 terrain and canopy heights in boreal forests. Remote Sensing of Environment 251, 112110. https://doi.org/10.1016/j.rse.2020.112110

Neuenschwander, A., Pitts, K., 2019. The ATL08 land and vegetation product for the ICESat-2 Mission. Remote Sensing of Environment 221, 247–259. https://doi.org/10.1016/j.rse.2018.11.005

[dataset] Neuenschwander, A.L., Pitts, K.L., Jelley, B.P., Robbins, J., Klotz, B., Popescu, S.C., Nelson, R.F., Harding, D., Pederson, D., Sheridan, R., 2021. ATLAS/ICESat-2 L3A land and vegetation height, version 5. NASA National Snow and Ice Data Center Distributed Active Archive Center, Boulder, Colorado USA. https://doi.org/10.5067/ATLAS/ATL08.005. 15/04/2022.

NGS Infocenter, 2021. Background: Why is NGS replacing NAD 83 and NAVD 88? [WWW Document]. National Geodetic Survey. URL https://geodesy.noaa.gov/datums/newdatums/background.shtml (accessed 12.02.2022)

Neumann, T.A., Martino, A.J., Markus, T., Bae, S., Bock, M.R., Brenner, A.C., Brunt, K.M., Cavanaugh, J., Fernandes, S.T., Hancock, D.W., Harbeck, K., Lee, J., Kurtz, N.T., Luers, P.J., Luthcke, S.B., Magruder, L., Pennington, T.A., Ramos-Izquierdo, L., Rebold, T., Skoog, J., Thomas, T.C., 2019. The Ice, Cloud, and Land Elevation Satellite – 2 mission: A global geolocated photon product derived from the Advanced Topographic Laser Altimeter System. Remote Sensing of Environment 233, 111325. https://doi.org/10.1016/j.rse.2019.111325

Painter, T.H., Berisford, D.F., Boardman, J.W., Bormann, K.J., Deems, J.S., Gehrke, F., Hedrick, A., Joyce, M., Laidlaw, R., Marks, D., Mattmann, C., McGurk, B., Ramirez, P., Richardson, M., Skiles, S.M., Seidel, F.C., Winstral, A., 2016. The Airborne Snow Observatory: Fusion of scanning lidar, imaging spectrometer, and physically-based modeling for mapping snow water equivalent and snow albedo. Remote Sensing of Environment 184, 139–152. https://doi.org/10.1016/j.rse.2016.06.018

[dataset] Painter, T. H. and K. J. Bormann. (2020). ASO L4 Lidar Point Cloud Digital Terrain Model 3m UTM Grid, Version 1 [Data Set]. Boulder, Colorado USA. NASA National Snow and Ice Data Center Distributed Active Archive Center. https://doi.org/10.5067/2EHMWG4IT76O. Date Accessed 11-29-2022.

Perovich, D.K., 2007. Light reflection and transmission by a temperate snow cover. Journal of Glaciology 53, 201–210. https://doi.org/10.3189/172756507782202919

Pflug, J.M., Margulis, S.A., Lundquist, J.D., 2022. Inferring watershed-scale mean snowfall magnitude and distribution using multidecadal snow reanalysis patterns and snow pillow observations. Hydrological Processes 36, e14581. https://doi.org/10.1002/hyp.14581

Riley, S.J., DeGloria, S.D., Elliot, R., 1999. A Terrain Ruggedness Index that Quantifies Topographic Heterogeneity. Intermountain Journal of Sciences 5, 1-4, 23-27.

Shean, D., Bhushan, S., Smith, B., Besso, H., Sutterley, T., Swinski, J.-P., Henderson, S., Neumann, T., Williams, J.B., 2021. Evaluating and improving seasonal snow depth retrievals with satellite laser altimetry 2021, C33B-04.

Shean, D., Swinski, J.P., Smith, B., Sutterley, T., Ugarte, C., Neumann, T., n.d. SlideRule: Enabling rapid, scalable, open science for the NASA ICESat-2 mission and beyond 6.

[dataset] Smith, B., Adusumilli, S., Csatho, B.M., Felikson, D., Fricker, H.A., Gardner, A., Holschuh, N., Lee, J., Nilsson, J., Paolo, F.S., Siegfried, M.R., Sutterley, T., and the ICESat-2 Science Team, 2021. ATLAS/ICESat-2 L3A Land Ice Height, Version 5. Boulder, Colorado USA. NASA National Snow and Ice Data Center Distributed Active Archive Center. https://doi. org/10.5067/ATLAS/ATL06.005. https://doi.org/10.5067/ATLAS/ATL06.005. 15/04/2022.

Smith, B., Fricker, H.A., Holschuh, N., Gardner, A.S., Adusumilli, S., Brunt, K.M., Csatho, B., Harbeck, K., Huth, A., Neumann, T., Nilsson, J., Siegfried, M.R., 2019. Land ice height-retrieval algorithm for NASA's ICESat-2 photon-counting laser altimeter. Remote Sensing of Environment 233, 111352. https://doi.org/10.1016/j.rse.2019.111352

Sochor, L., Seehaus, T., Braun, M.H., 2021. Increased Ice Thinning over Svalbard Measured by ICESat/ICESat-2 Laser Altimetry. Remote Sensing 13, 2089. https://doi.org/10.3390/rs13112089

[dataset] Swinski, JP., Shean, D., Sutterley, T., 2022. ICESat2-SlideRule/sliderule-icesat2: v1.4.2 (v1.4.2). Zenodo. https://doi.org/10.5281/zenodo.6565071

Treichler, D., Kääb, A., 2017. Snow depth from ICESat laser altimetry — A test study in southern Norway. Remote Sensing of Environment 191, 389–401. https://doi.org/10.1016/j.rse.2017.01.022

Walker, C.C., Becker, M.K., Fricker, H.A., 2021. A High Resolution, Three-Dimensional View of the D-28 Calving Event From Amery Ice Shelf With ICESat-2 and Satellite Imagery. Geophysical Research Letters 48, e2020GL091200. https://doi.org/10.1029/2020GL091200

Wang, C., Wang, C., Wang, C., Zhu, X., Zhu, X., Zhu, X., Nie, S., Nie, S., Nie, S., Xi, X., Li, D., Zheng, W., Chen, S., 2019. Ground elevation accuracy verification of ICESat-2 data: a

case study in Alaska, USA. Opt. Express, OE 27, 38168–38179. https://doi.org/10.1364/OE.27.038168
Warren, S.G., 2019. Optical properties of ice and snow. Philos Trans A Math Phys Eng Sci 377, 20180161. https://doi.org/10.1098/rsta.2018.0161
Washington State Department of Natural Resources, 2018. Lidar Project Quality Assurance Report. Washington Geologic Survey.
[dataset] Atlantic 2018 Leaf-On LiDAR Data Acquisition, 2018. WA DNR Methow Basin DTM 2018. https://lidarportal.dnr.wa.gov/
Zhang, Y., Pang, Y., Cui, D., Ma, Y., Chen, L., 2021. Accuracy Assessment of the ICESat-2/ATL06 Product in the Qilian Mountains Based on CORS and UAV Data. IEEE Journal of Selected Topics in Applied Earth Observations and Remote Sensing 14, 1558–1571. https://doi.org/10.1109/JSTARS.2020.3044463

Supplemental

Table S-1

Comparison of ATL06SR-ALS pairs. **IS** stands for ICESat-2, **At** stands for track ASO data, and **Ab** stands for basin ASO data.

	Pair 1			Pair 2			Pair 3			Pair 4			Pair 5			Pair 6			Pair 7			Pair 8			All Pairs		
	IS	**At**	**Ab**	**IS**	**At**	**Ab**	**IS**	**At**	**Ab**	**IS**	**At**	**Ab**	**IS**	**At**	**Ab**	**IS**	**At**	**Ab**	**IS**	**At**	**Ab**	**IS**	**At**	**Ab**	**IS**	**At**	**Ab**
Date Offset	**12**			**7**			**11**			**6**			**17**			**17**			**2**			**2**			9		
Median Depth (m)	2.83	2.98	2.84	2.45	2.56	2.54	1.6	2.04	1.72	1.3	1.02	0.98	0.04	0	0.01	0.85	1.07	1.05	0.89	1.12	1.04	0.59	0.59	0.51	1.09	1.04	1.04
Difference Between Medians		0.16	-0.01		0.11	-0.09		-0.44	-0.12		-0.28	0.31		0.04	0.03	0.22	-0.2			-0.23	-0.15		0	0.08		0.19	0.11
% Difference Between Medians		5	0		4	-4		-22	-7		-27	32		inf	281		21	-19		-21	-15		0	16		21	15
IQR (m)	2.91	2.6	1.71	1.25	1.02	1.89	1.78	1.15	1.99	1.42	0.84	1.18	1.31	0.3	0.34	1.18	0.37	0.71	1.52	0.52	0.67	0.79	0.45	0.79	0.68	0.6	0.99
% Difference Between IQRs		-12	70		-22	-34		55	-11		-69	20		340	289		-219	67		191	127		-75	0		72	50
delta TUM (m)	-0.2			-0.15			-0.64			-0.25			0.03			-0.03			-0.03			-0.08			0.11		
delta DAN (m)	-0.15			NaN			-0.33			NaN			0			0.2			0			-0.05			0.1		